

TWO-DIMENSIONAL NUMERICAL SIMULATION OF A FREE FALL CYLINDER USING THE IMMERSED BOUNDARY METHOD WITH THE VIRTUAL PHYSICAL MODEL

Alessandra Costa Vilaça

Laboratory of Heat and Mass Transfer and Fluid Dynamic – University Federal of Uberlândia
Mechanical Engineer College – Bloco 1M – Av. João Naves de Ávila, 2.121. CEP 38400-902
ailevica@yahoo.com

José Eduardo Santos Oliveira

jeolivei@mecanica.ufu.br

Ana Lúcia Fernandes de Lima e Silva

alfsilva@mecanica.ufu.br

Aristeu Silveira Neto

aristeus@mecanica.ufu.br

Abstract. *The present work shows the two-dimensional results of the numerical simulations of a free fall cylinder using the Immersed Boundary (IB) method (Peskin, 1977). In the IB method a Lagrangian grid is used to represent the immersed body and a Cartesian Eulerian grid represents the discretized domain. The force term added to the Navier Stokes is calculated with the Virtual Physical Model (VPM) (Lima e Silva, 2002), which is based on the solution of the movement equations over the Lagrangian grid. The great advantage of the IB method is the possibility of simulate moving or deformable bodies without the need of remesh the domain. The numerical results such as the terminal velocity and the forces acting over the cylinder are presented and compared with the analytical results. The comparison shows good agreement and results reproduces the expected physical behavior.*

Keywords: *free fall, immersed body, cylinder, virtual physical model*

1. Introduction

One of the first works about free fall of particles in Newtonian fluids was reported by Newton (1760). Since then the study of the movement of particles in Newtonians and non Newtonians fluids is being the focus of researches along the centuries. The knowledge of the interaction solid-fluid is of a great of importance for the understanding of the fluid dynamics. These interactions can influence the mean velocity, the aggregation rate, the density of the fluid, the lubricating effects of the fluid on the particles, the paths of the particles, therefore they are important for the understanding of the flow dynamics. The knowledge of the particle path is important for different industrial areas such as sedimentation, meteorology, aerospace engineering, biology, etc (Bönisch and Heuveline, 2004). The movement of suspended particles in a fluid is studied for example, in composed materials, ceramic, polymeric, flocculation processes, fluidization, sedimentation, dynamics of blood cells and other.

In the last decades a great interest has been demonstrating in classifying and to quantifying different types of movements of free fall for different regimes. Maybe because of the lack of information in the literature that difficult the knowledge of the interaction solid-fluid and of the fluid dynamics. The qualitative analysis of the occurrence of formation of vortexes and its influence in the movement of the body is still a subject discussing. For the quantitative analysis, the determination of the transition among different fall regimes for bodies with different geometries, is still also a challenge.

The present work uses the Immersed Boundary (IB) method with the Virtual Physical Model (VPM) proposed by Lima e Silva *et al.* (2003). The base of this methodology consists of working with a Cartesian grid to represent the domain and a Lagrangian grid for the immersed particle. The force field models the presence of the immersed interface, guaranteeing the imposition of the desired boundary conditions on the particle surface. The VPM is a new alternative for the calculation of the force field added to the Navier-Stokes equations. It is worth to point out that this methodology, which allows simulating flows with particles of any geometric shape and also with moving particles. The simulations were carried out for a free fall cylindrical particle at different regimes. The results of terminal velocity and forces acting on the particle were obtained. The temporal vortex formation above the critical Reynolds number is presented. The numerical terminal velocity was compared with the analytic results. A summarized description of the mathematical formulation is shown in the next item and more details can be found in Lima e Silva, (2003).

2. Immersed Boundary Method with Virtual Physical Model

The Immersed Boundary method uses a Eulerian grid and a Lagrangian grid such as represented in Fig. 1. The meshes are geometrically independent and the force field calculated on the interface is responsible for the coupling and for the change of information among the grids.

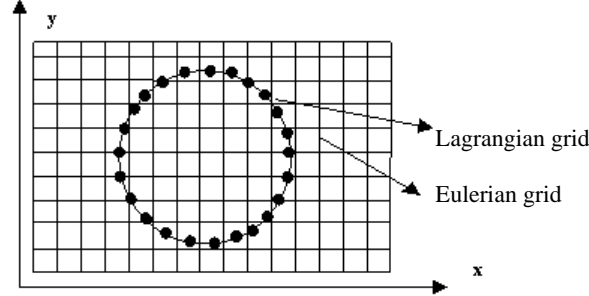


Figure 1. Schematic view of the Eulerian and the Lagrangian grid.

The Navier Stokes equations for a two-dimensional incompressible flow can be written as:

$$\rho \left[\frac{\partial u_i}{\partial t} + \frac{\partial(u_i u_j)}{\partial x_j} \right] = -\frac{\partial P}{\partial x_i} + \frac{\partial}{\partial x_j} \left(\mu \left(\frac{\partial u_i}{\partial x_j} + \frac{\partial u_j}{\partial x_i} \right) \right) + f_i \quad (1)$$

$$\frac{\partial u_j}{\partial x_j} = 0 \quad (2)$$

where f_i is the Eulerian force calculated by:

$$f_i = \sum D(\vec{x} - \vec{x}_k) F(\vec{x}, t) \Delta s^2(\vec{x}_k) \quad (3)$$

\vec{x} and \vec{x}_k are the Eulerian and the Lagrangian coordinate vectors, Δs is the distance between two Lagrangian points and $D(\vec{x} - \vec{x}_k)$ is the interpolation/distribution function with Gaussian properties given by:

$$D = \frac{f \left[(x_k - x_i) / h \right] f \left[(y_k - y_j) / h \right]}{h^2} \quad (4)$$

$$f(r) = \begin{cases} f_1(r) & \text{se } \|r\| < 1 \\ \frac{1}{2} - f_1(2 - \|r\|) & \text{se } 1 < \|r\| < 2 \\ 0 & \text{se } \|r\| > 2 \end{cases} \quad (5)$$

$$f_1(r) = \frac{3 - 2\|r\| + \sqrt{1 + 4\|r\| - 4\|r\|^2}}{8} \quad (6)$$

where r represents $(x_k - x_i) / h$ or $(y_k - y_j) / h$, h is the Eulerian mesh size and (x_i, y_i) is the Eulerian coordinates vector, represented in Fig. 2.

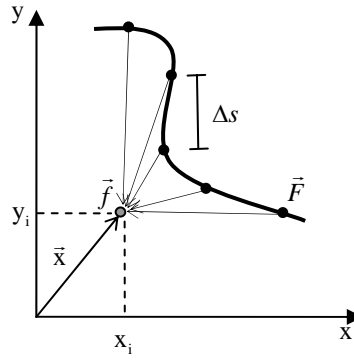


Figure 2. Lagrangian force distribution for a Eulerian point.

The Eulerian force \vec{f} is different from zero only on the interface and in its neighborhood.

The VPM proposed by Lima e Silva *et al.* (2003) for the Lagrangian force calculation is based on the solution of the moment equations over the volumes of fluid centered on the Lagrangian points. The Lagrangian force is obtained by:

$$\vec{F}(\vec{x}_k, t) = \underbrace{\rho \frac{\partial \vec{V}(\vec{x}_k, t)}{\partial t}}_{\vec{F}_a} + \underbrace{\rho \vec{V}(\vec{x}_k, t) \cdot \vec{V}(\vec{x}_k, t)}_{\vec{F}_i} - \underbrace{\mu \nabla^2 \vec{V}(\vec{x}_k, t)}_{\vec{F}_v} + \underbrace{\vec{\nabla} p(\vec{x}_k, t)}_{\vec{F}_p} \quad (7)$$

The terms of Eq. (7) are named the acceleration force \vec{F}_a , the inertial force \vec{F}_i , the viscous force \vec{F}_v and de pressure force \vec{F}_p . These terms are calculated on the Lagrangian grid points using the pressure and velocity fields from the Eulerian grid. The derivatives are calculated by the interpolation of the Eulerian variables on Lagrangian auxiliary points using the interpolation function given by Eqs. (4), (5) and (6). After this, a Lagrange polynomial is used for the derivatives calculation.

3. Numerical Method

For the numerical solution of the incompressible Navier-Stokes the non-interactive Fractional Step method (Kim and Moin, 1985) was used. The second order Finite difference method for staggered grids was applied for the spatial discretization and the explicit second order Runge-Kutta method for the temporal discretization. The linear system generated by the discretization of the Poisson equation for the correction pressure was solved by the Modified Strongly Implicit Procedure (MSI) (Schneider and Zedan, 1981).

4. Forces acting on a free fall cylinder particle

The free fall of a two-dimensional cylinder in an infinite medium can be characterized by the forces acting over its surface. At the beginning the fluid is in rest and the particle begins to move due to the resultant of the forces represented in Fig. 3. The particle moves in the descending direction if the force weight is larger than the sum of the drag and the buoyancy forces.

The resultant force can be obtained by:

$$\vec{F}_R = \vec{F}_d + \vec{F}_b - \vec{F}_w \quad (8)$$

where \vec{F}_d is the drag force, \vec{F}_w is the weight force and \vec{F}_b the buoyancy force. Applying the second Newton's law:

$$\vec{F}_R = m_p \vec{a} \quad (9)$$

where m_p is the particle mass and \vec{a} its acceleration. Equations (8) and (9) can be equaled:

$$m_p \vec{a} = \vec{F}_d + \vec{F}_b - \vec{F}_w \quad (10)$$

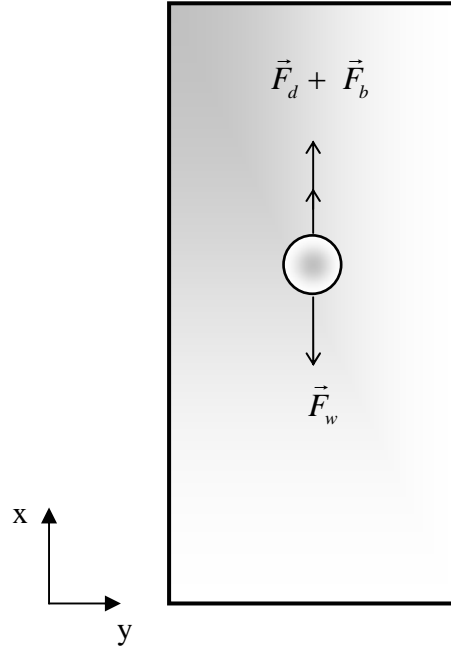


Figure 3. Forces acting on a two-dimensional cylindrical particle.

The buoyancy force, \vec{F}_b , can be written by:

$$\vec{F}_b = \rho_f g V_p \quad (11)$$

where ρ_f is the fluid density, V_p is the particle volume and g the acceleration of gravity. The drag force is the component of the force acting parallel to the direction of the fluid movement, F_d . This force is the y component of the Lagrangian force obtained directly from the VPM. The weight force due to the gravity action is:

$$\vec{F}_w = \rho_p g V_p \quad (12)$$

where ρ_p is the particle density. The particle acceleration can be written as:

$$\vec{a} = \frac{d\vec{V}_p}{dt} \quad (13)$$

Substituting Eqs. (11), (12) and (13) in Eq. (10) the particle velocity (V_p) can be obtained. The discretized equation of the particle velocity depends on the previous time velocity and the drag, weight and buoyancy forces. It can be written as:

$$V_p^{n+1} = V_p^n + \frac{\Delta t}{\rho_p} \left[g_y (\rho_p - \rho_f) - \frac{F_d}{V_p} \right] \quad (14)$$

5. Results

For the present simulations a non-uniform grid was used to discretize the domain represent in Fig. 4. The square region, which involves the cylinder, has uniform mesh due to the force distribution process. The cylinder has diameter $d = 0.01$ m and is located at (0.15, 0.2). The Neumann boundary conditions for the velocity are used. At the inlet a prescribed uniform velocity profile was applied. The fluid properties are density equal to 1.0 Kg/m^3 and viscosity equal to $1.0 \times 10^{-4} \text{ Kg/(m.s)}$. Instead of to displace the particle inside the domain the inlet velocity is changed in accordance with the dynamic model proposed by Eq. (14) obtained through the forces balance acting on a particle. This procedure only change the referential maintaining the flow dynamics as the same.

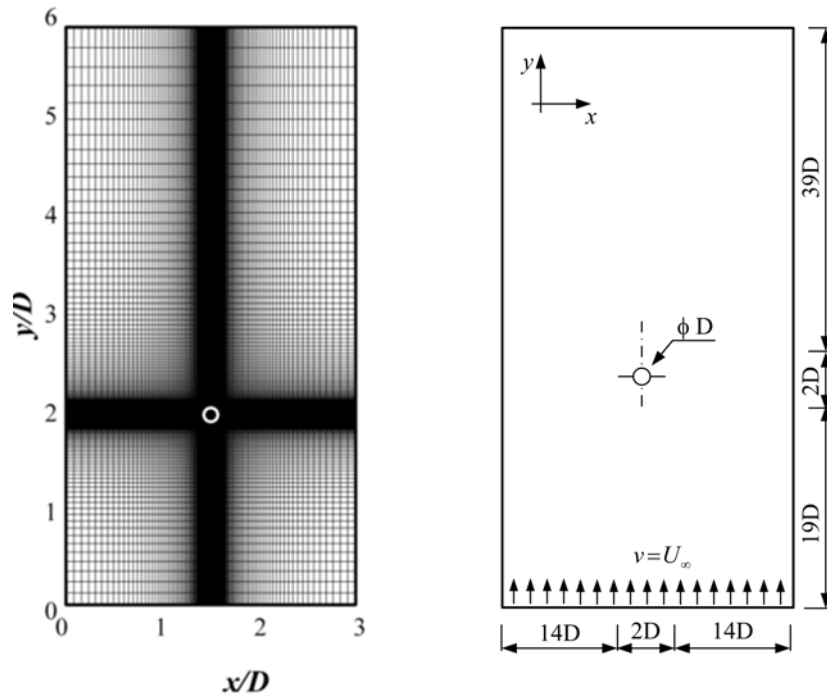


Figure 4. Illustration of the domain.

5.1. Laminar Regime

This simulation was carried out for a particle of density 3.0 Kg/m^3 and viscosity $1.0 \times 10^{-4} \text{ Kg/(m.s)}$. The Lagrangian grid has 320 points and the Eulerian grid 16920 points. At the beginning a uniform velocity profile of $v = 0.01 \text{ m/s}$ which corresponds $Re = 1$. The Reynolds number at the end of the simulation is 41.131. Figure 5 shows sum of the buoyancy and drag forces compared with the weight force. It can be observed the good agreement when the particle velocity reaches terminal velocity.

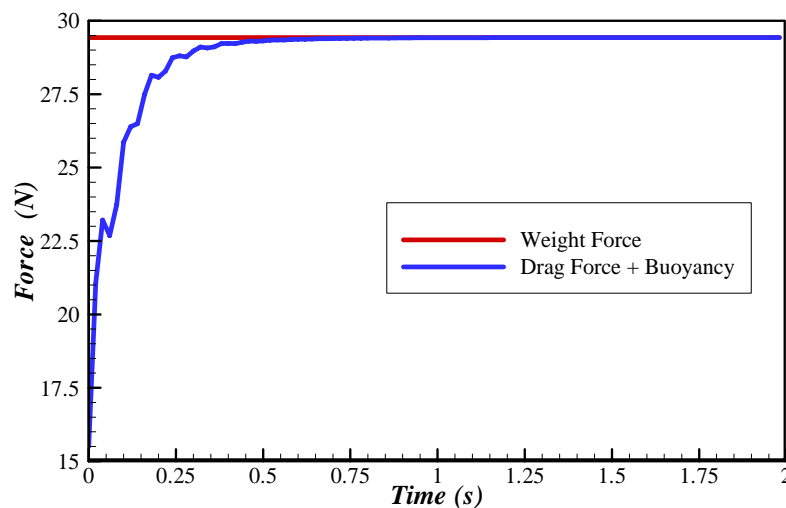


Figure 5. Drag and buoyancy forces as a function of time compared with the weight force.

The numerical terminal velocity obtained for the present simulation was of 0.4113 m/s . The time of 0.25221 s corresponds the time which this terminal velocity was reached. Figure 6 compares the numerical terminal velocity with the analytical velocity. The difference between the values is of 0.63% .

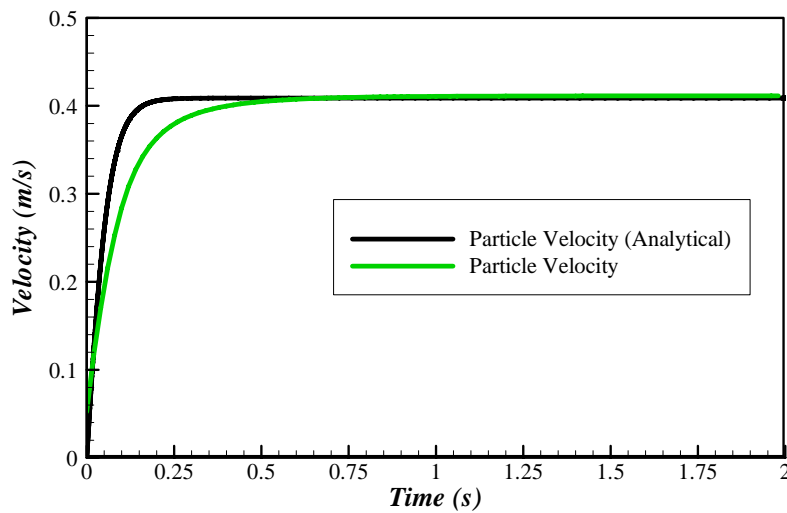


Figure 6. Numerical terminal velocity compared with the analytical result.

The analytical terminal velocity was calculated by integration using Runge-Kutta second order of analytical equation obtained through the forces balance acting on a cylindrical particle. The drag coefficient was calculated by correlation presented in Eq. (15).

$$Cd = 1 + \frac{10}{Re^{2/3}} \quad (15)$$

4.2. Instable Regime

For this simulation a particle of density 10.0 Kg/m^3 and viscosity $1.0 \times 10^{-4} \text{ Kg/(m.s)}$. The domain of dimensions is the same of was used previously in Fig. 4. The boundary conditions are the same of the last simulated case.

The initial Reynolds number is also equal to 1 and at the end of the simulation $Re = 100$. The terminal velocity for this case was 0.942 m/s for a time of 0.1524 s . The terminal Reynolds number for this simulation is higher than the critical Reynolds number ($Re_c \cong 47$).

Figure 7 presents the temporal evolution of the forces and of the terminal velocity. The analytical velocity is also showed. The temporal development of the bubble of recirculation could be visualized through the streamlines in Fig. 8 at the same instants (1), (2), (3), (4), (5) and (6) showed in Fig. 7.

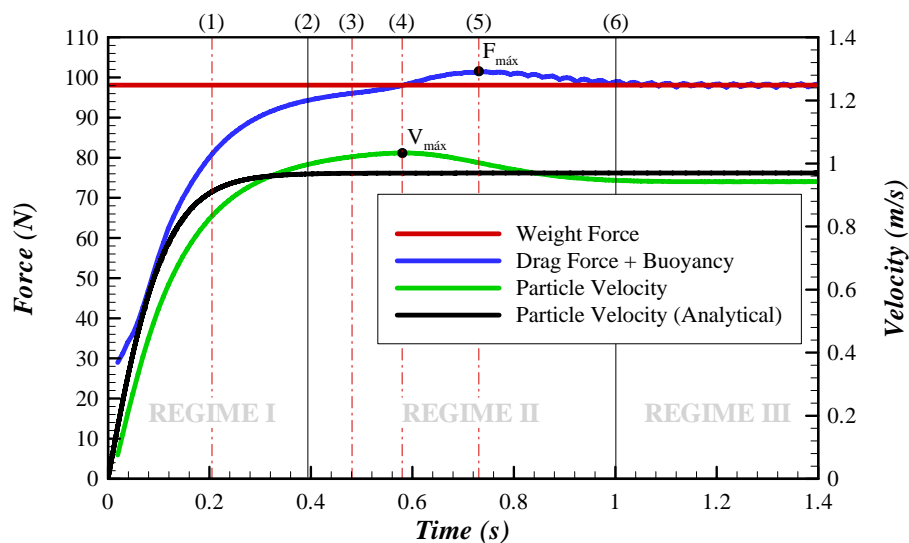


Figure 7. Velocity and forces acting on the cylinder as a function of time.

The regime I (that involves points 1 and 2) can be named laminar regime because the recirculation bubble is symmetric to the y axis. At the point 2 the bubble reaches its maximum size and starts to oscillate the vortex shedding. At point 3 the bubble starts to prolong asymmetrically. The particle velocity is maximum at point 4 where the resultant force is zero and the acceleration is null. Regime II is characterized by asymmetry of the recirculation bubble and the beginning of the vortex shedding which are still prolonged. At point 5 the drag force increases due to the negative acceleration until point 6 where the resultant force is zero and the particle velocity is constant. At point 6 the terminal velocity was reached and the regime III has a constant mean frequency of vortex shedding.

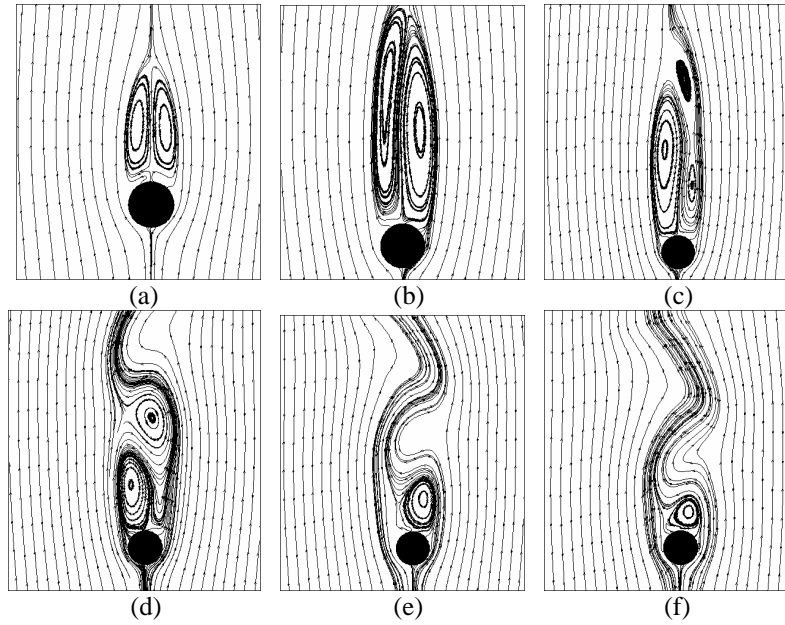


Figure 8. Temporal evolution recirculation bubble: point 1 (a), point 2 (b), point 3 (c), point 4 (d), point 5 (e) and point 6 (f) according to Fig. 7.

Figure 9 shows the results obtained with the simulation for a cylinder of $\rho_p = 60 \text{ kg/m}^3$. The domain, the initial and boundary conditions are the same as the previous cases. The terminal Reynolds number is 250. For these conditions the weight force is approximately six times higher than the last simulated case. Figure 10 presents the temporal evolution of the recirculation bubble at the time instants represented in Fig. 9.

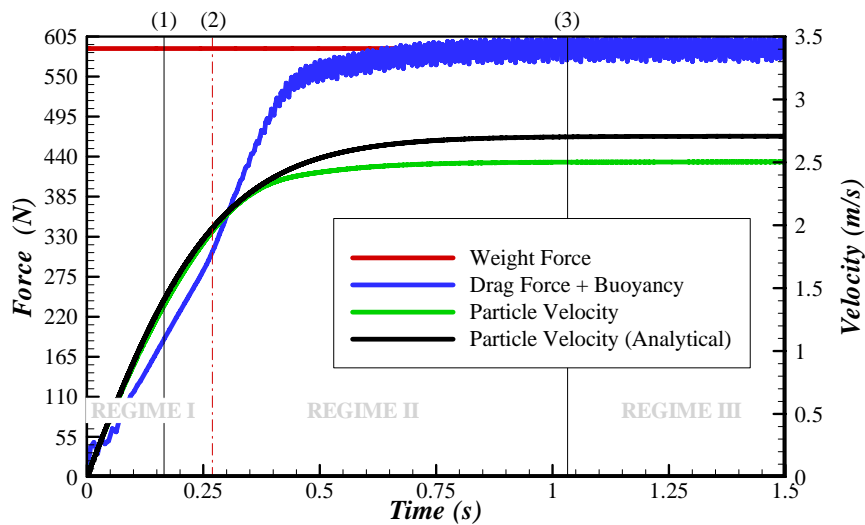


Figure 9. Velocity and forces acting on the cylinder as a function of time.

For this simulation the regime I (point 1) is characterized by a symmetric recirculation bubble when the bubble size is maximum. At point 1 the Reynolds number is approximately 100 as the same final value from the last simulation. At point 2 the bubble is asymmetric and the vortex shedding starts. In this point the drag force and buoyancy presents the higher slope. The weight force is still higher than the sum of drag and buoyancy. In this case, the particle is six times heavier than the particle the last simulation. The regime II is characterized for a prolonged and asymmetric bubble. The particle velocity is maximum at point 3, which starts the regime III. In this regime the particle velocity is constant and the vortex shedding has a standard behavior. The difference between the values the numerical terminal velocity with the analytical velocity is 8.14%.

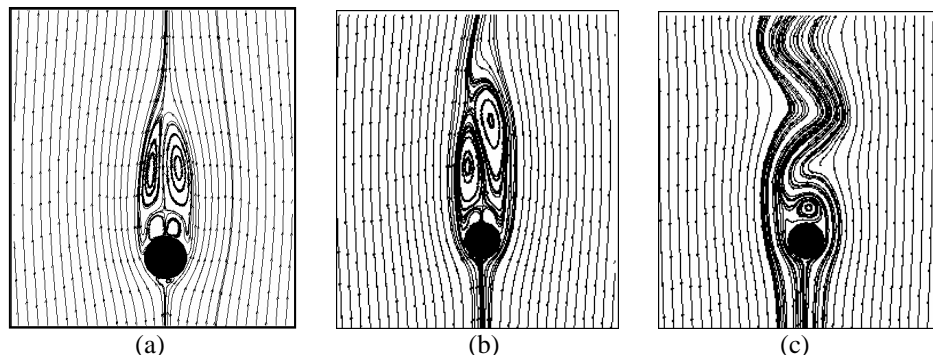


Figure 10. Temporal evolution of the recirculation bubble. Point 1 (a), point 2 (b) and point 3 (c) according to Fig. 9.

5. Conclusions

The simulation results of a free fall cylindrical particle were presented and compared with the analytical results. The comparison presented good agreement showing the capability to simulated moving single bodies. The temporal results provided different regimes of flows characterized by the vortex dynamic, the values of the forces and velocity provided a satisfactory and coherent behavior when compared a physical behavior expected. The next step of this work is a new implementation that will allow the movement of rotation and translation of the cylinder that characterize the fluid-structure interaction.

6. Acknowledgements

The authors acknowledge CNPq (National Council for Scientific and Technological Development, from Brazilian Ministry of Education) and Fapemig (Foundation for the Support of Research in Minas Gerais, Brazil) for the financial support and the Mechanical Engineering College of the Federal University of Uberlândia.

7. References

- Bönisch S. and Heuveline, V., 2004, "On the Numerical Simulation of the Instationary Free Fall of a Solid in a Fluid. I. The Newtonian case", Technical Report 2004-24, University Heidelberg, 22 p.
- Kim, J. e Moin, P., 1985, "Application of a Fractional Step Method to Incompressible Navier-Stokes Equations", Journal Computational Physics, Vol. 59, 308 p.
- Lima and Silva, A.L.F, 2002, Desenvolvimento e implementação de uma nova metodologia para modelagem de escoamentos sobre geometrias complexas: Método da Fronteira Imersa com Modelo Físico Virtual, Tese de doutorado em Engenharia Mecânica, Universidade Federal de Uberlândia, MG, Brasil.
- Lima and Silva, A. L. F., Silveira-Neto, A. and Damasceno, J. J. R., 2003, "Numerical Simulation of Two Dimensional Flows over a Circular Cylinder using the Immersed Boundary Method", Journal of Computational Physics, Vol. 189, pp. 351-370.
- Newton, I., 1760, "Philosophia Naturalis: Principia Mathematica", Coloniae Allobrookum, Roma.
- Peskin, C. S., 1977, "Numerical Analysis of Blood Flow in the Heart", J. Comp. Phys., Vol. 25, pp. 220.
- Schneider, G. E. and Zedan, M., 1981, "A Modified Strongly Implicit Procedure for the Numerical Solution of Field Problems", Numerical Heat Transfer, Vol.4, pp. 1-19.

8 Responsibility notice

The authors are the only responsible for the printed material included in this paper.